Numerical Analysis of Tracking Performance in Machine Tools for Disturbance Forces Compensation Using PID And NPID Controller

Submitted By

ABDULSALAM MANSOOR, 190011131

ABDULFATAH KHMEES, 190011129

MOGTABA ELSER, 180011248

Supervised By

Dr. Madihah Binti Haji Maharof

A Thesis Submitted in Partial Fulfillment of the Requirement for the Degree of Bachelor of Science in Mechanical Engineering

Department of Mechanical and Production Engineering (MPE)

Islamic University of Technology (IUT)

January, 2024

CERTIFICATE OF RESEARCH

This thesis titled ***"Numerical Analysis of Tracking Performance in Machine Tools for Disturbance Forces Compensation Using PID And NPID Controller"*** *submitted by Abdulsalam Mansoor (190011131), Abdulfatah Khmees (190011129), and Mogtaba Elser (180011248) has been accepted as satisfactory in partial fulfillment of the requirement for the Degree of Bachelor of Science in Mechanical Engineering.*

Supervisor

Dr. Madihah Binti Haji Maharof
Assistant Professor

Head of the Department

Dr. Md Hamidur Rahman
Professor

Department of Mechanical and Production Engineering (MPE)
Islamic University of Technology (IUT)

DECLARATION

I hereby declare that this thesis report entitled ***"Numerical Analysis of Tracking Performance in Machine Tools for Disturbance Forces Compensation using PID and NPID Controller"*** *is an authentic report of study carried out as a requirement for the award of degree B.Sc. (Mechanical Engineering) at Islamic University of Technology, Gazipur, Dhaka, under the supervision of Dr. Madihah Binti Haji Maharof, Assistant Professor, MPE, IUT in the year 2024*

The matter embodied in this thesis has not been submitted in part or full to any other institute for award of any degree.

_____

Abdulsalam Mansoor

190011131

_____

Mogtaba Elser

180011248

_____

Abdulfatah Khmees

190011129

PO Mapping of ME 4800 -Thesis and Project

COs	Course Outcomes (CO) Statement	(PO)	Addressed by	
CO1	Discover and Locate research problems and illustrate them via figures/tables or projections/ideas through field visit and literature review and determine/Setting aim and objectives of the project/work/research in specific, measurable, achievable, realistic and timeframe manner.	**PO2**	Thesis Book	
			Performance by research	
			Presentation and soft skill	
CO2	Design research solutions of the problems towards achieving the objectives and its application. Design systems, components or processes that meets related needs in the field of mechanical engineering	**PO3**	Thesis Book	
			Performance by research	
			Presentation and soft skill	
CO3	Review, debate, compare and contrast the relevant literature contents. Relevance of this research/study. Methods, tools, and techniques used by past researchers and justification of use of them in this work.	**PO4**	Thesis Book	
			Performance by research	
			Presentation and soft skill	
CO4	Analyse data and exhibit results using tables, diagrams, graphs with their interpretation. Investigate the designed solutions to solve the problems through case study/survey study/experimentation/simulation using modern tools and techniques.	**PO5**	Thesis Book	
			Performance by research	
			Presentation and soft skill	
CO5	Apply outcome of the study to assess societal, health, safety, legal and cultural issue and consequent possibilities relevant to mechanical engineering practice.	**PO6**	Thesis Book	
			Performance by research	
			Presentation and soft skill	
CO6	Relate the solution/s to objectives of the research/work for improving desired performances including economic, social and environmental benefits.	**PO7**	Thesis Book	
			Performance by research	
			Presentation and soft skill	
CO7	Apply moral values and research/professional ethics throughout the work, and justify to genuine referencing on sources, and demonstration of own contribution.	**PO8**	Thesis Book	
			Performance by research	
			Presentation and soft skill	
CO8	Perform own self and manage group activities from the beginning to the end of the research/work as a quality work.	**PO9**	Thesis Book	
			Performance by research	
			Presentation and soft skill	
CO9	Compile and arrange the work outputs, write the report/thesis, a sample journal paper, and present the work to wider audience using modern communication tools and techniques.	**PO10**	Thesis Book	
			Performance by research	
			Presentation and soft skill	
CO10	Organize and control cost and time of the work/project/research and coordinate them until the end of it.	**PO11**	Thesis Book	
			Performance by research	
			Presentation and soft skill	
CO11	Recognize the necessity of life-long learning in career development in dynamic real-world situations from the experience of completing this project.	**PO12**	Thesis Book	
			Performance by research	
			Presentation and soft skill	

Student Name /ID:

1. Abdulsalam Mansoor, 190011131

2. Mogtaba Elser, 180011248

3. Abdulfatah Khmees, 190011129

Signature of the Supervisor:

Name of the Supervisor:

K-P-A Mapping of ME 4800 -Thesis and Project

COs	POs	Related Ks								Related Ps							Related As				
		K1	K2	K3	K4	K5	K6	K7	K8	P1	P2	P3	P4	P5	P6	P7	A1	A2	A3	A4	A5
CO1	PO2																				
CO2	PO3																				
CO3	PO4																				
CO4	PO5																				
CO5	PO6																				
CO6	PO6																				
CO7	PO8																				
CO8	PO9																				
CO9	PO10																				
CO10	PO11																				
CO11	PO12																				

Student Name /ID:

1. Abdulsalam Mansoor, 190011131

2. Mogtaba Elser, 180011248

3. Abdulfatah Khmees, 190011129

Signature of the Supervisor:

Name of the Supervisor:

ACKNOWLEDGEMENT

In the Name of Allah, the Most Beneficent, the Most Merciful

First of all, we are grateful to ALLAH (SWT), the most benevolent and kind for providing us the strength and ability to write this dissertation. we want to thank our project supervisor, Dr. Madihah Binti Haji Maharof, for her strong and patient support through unpredictable problems during the project and her precious advice when we faced difficulties. Her generosity, kindness, and strong supervision during work made us feel less stressed in confronting unexpected troubles and be more productive in our personal and academic life. Finally, we would like to acknowledge gratefully for the financial support by The Organization of Islamic Cooperation (OIC).

ABSTRACT

In modern production, machine tool precision and reliability are critical for producing high-quality goods. To meet these objectives, numerous new controllers and control algorithms have been developed, taking use of technological advancements. One key problem in preserving product quality is managing internal disturbances induced by cutting and friction forces, which can have a considerable impact on finish quality. Recent research has provided novel approaches to addressing these difficulties through improved control mechanisms.This study investigates the efficiency of nonlinear proportional-integral-derivative (NPID) controllers over typical PID controls for reducing tracking errors in machining operations. The study begins with a complete system identification procedure to precisely represent the machine tool system, which is required for effective controller design. By comparing the performance of NPID and PID controllers, the study hopes to provide insights into the best strategies for accomplishing precise and efficient machining operations, resulting in higher product quality. In the MATLAB and Simulink simulations, perturbation forces were applied at frequencies of 0.2 Hz and 0.4 Hz, with spindle speeds of 1500 rpm and 2500 rpm. At 0.2 Hz, the PID controller had maximum tracking errors (MTE) of 0.09990 mm and 0.09920 mm, which corresponded to error percentages of 0.66600% and 0.66100%. At 0.4 Hz, the MTEs were 0.17600 mm and 0.17500 mm, with error percentages of 1.17300% and 1.16600%. The NPID controller, on the other hand, demonstrated MTEs of 0.09993 mm and 0.09927 mm at 0.2 Hz, yielding error percentages of 0.66620% and 0.66180%, respectively. At 0.4 Hz, the NPID controller measured MTEs of 0.17660 mm and 0.17520 mm, with error percentages of 1.17730% and 1.16800%. The Root Mean Square Error (RMSE) statistics emphasized the performance variations amongst the controllers. The PID controller had RMSE values of 0.06958 mm at 1500 rpm, 0.06960 mm at 2500 rpm at 0.2 Hz, and 0.12410 mm at both speeds at 0.4 Hz. The NPID controller had RMSE values of 0.06954 mm at 1500 rpm, 0.06956 mm at 2500 rpm at 0.2 Hz, and 0.12380 mm at both speeds at 0.4 Hz. The results show that the NPID controller consistently beat the PID controller in terms of tracking error and RMSE minimization. This shows that the NPID controller provides more precision and better performance during machining processes.

TABLE OF CONTENTS

LIST OF TABLES

LIST OF FIGURES

LIST OF ABBREVIATIONS

CNC	-	Computer Numerical
PID	-	Proportional-Integral-Derivative
NPID	-	Nonlinear Proportional-Integral-Derivative
P/PI	-	Proportional/Proportional-Integral
SMC	-	Sliding Mode Control
DAC	-	Digital-to-Analog Converter
ADC	-	Analog-to-Digital Converter
MTE	-	Maximum Tracking Error
RMSE	-	Root Mean Square Error
NCasFF	-	Nonlinear Cascade Feedforward
FFT	-	Fast Fourier Transform
P	-	Proportional
ZPETC	-	Zero Phase Error Tracking Controller
CCC	-	Cross Coupling Controller
MBDA	-	Model-Based Disturbance Attenuator
DOB	-	Disturbance Observer
SARC	-	Simplified Adaptive Robust
QFT	-	Quantitative Feedback Theory
RLS	-	Recursive Least Squares
MRC	-	Model Reference Control
GMS	-	Generalized Maxwell-Slip
DADSC	-	Disturbance Adaptive Discrete-Time Sliding Mode Controller
AFC	-	Adaptive Feed-Forward
PPC+LS	-	Pole Placement Controller and Loop Shaping
MPC	-	Model Predictive Control
FSMC	-	Fuzzy Sliding Mode Control

LIST OF SYMBOLS

V	-	Voltage
N	-	Rotational spindle speed of cutter
v	-	Cutting speed or feed rate
π	-	Pi
d	-	Diameter of the cutter
f	-	Feed per tooth
n	-	Number of teeth on the cutter
Fc	-	Cutting Force
Pc	-	Cutting Power
Gm	-	Transfer function of system model
NP	-	Nonlinear proportional gain
NI	-	Nonlinear integral gain
KP	-	Proportional gain
KI	-	Integral gain
KD	-	Derivative gain
S(jω)	-	Sensitivity
L	-	Open loop of the control system
e(t)	-	Tracking error
t	-	Time
f	-	Frequency
u_s	-	Minimum cutting force value
$u_{i,sat}$	-	Maximum input force value
R(s)	-	Input voltage
Z(s)	-	Position of the XYZ Ball Screw Drive Table

CHAPTER 1

INTRODUCTION

1.1 Introduction

A power-driven tool used in milling, turning, shearing, and grinding operations to cut and remove materials is called a machine tool. For materials to be shaped into products, especially intricate ones like satellites and aircraft components, machine tools are essential. These come in a variety of sizes and styles, with CNC milling machines being a popular choice in industry. In order to fulfill the increasing demand for extremely precise components, researchers are working on control system advancements to enhance machining speed, efficiency, and accuracy, especially with CNC machines. Machine tools, especially CNC machines, function differently when subjected to disturbance forces during machining. In machining operations, disturbance forces like cutting and friction forces are frequent and can have a detrimental effect on precision and accuracy. A XYZ ball screw drive table, which consists of two axis tables for workpiece placement and a single axis actuator for the Z-axis, duplicates the same cutting operation in addition to the CNC machine. Every table includes a ball screw shaft and servo motor for rotation. Cutting depth is exclusively controlled by the Z-axis, which is the only axis having a cutting tool and spindle. PID, NPID, P/PI, SMC, FLC, and other control systems are among those that the XYZ ball screw drive table may employ. These methods are coupled with the machine through the use of mathematical software, Digital-to-Analog Converters (DAC), and Analog-to-Digital Converters (ADC).

1.2 Problem Statements

Machine tool technologies have to keep up with the strict demands of accuracy, speed, and robustness. The intricate interaction of several elements such as workpiece mass, friction, cutting forces, and mechanical structure is what determines machine tool

precision. Mechanical resonances and vibrations caused by structural problems have been shown to impair tracking performance by adversely affecting the system's dynamics and frequency response. Furthermore, it becomes difficult to regulate performance when the mass of the work piece is greater than the mass of the work table, requiring the employment of stronger controls. Moreover, tracking and contour performance are hampered by unwanted nonlinear friction forces that result from interactions between the motor and the support bearing during velocity variations. High-frequency dynamic components are present in the effect of cutting forces, which function as input disturbances during machining and necessitate adjustment. Motion controllers that can effectively counteract disturbance forces must be carefully chosen if accurate motion is to be achieved in servo drive positioning systems. With the ultimate goal of increasing tracking accuracy and enhancing performance in machining processes, this research attempts to address these difficulties by pushing the limits of machine tool technology through creative control strategies and design considerations.

1.3 Objectives

The objectives of this research are:

i. To design a PID and NPID controller for a milling table ball screw-driven system.

ii. To validate numerically effect of cutting forces in the milling process using PID and NPID controller.

1.4 Scopes

The scopes of this research are:

i. Numerical validation and control design using MATLAB/Simulink software.

ii. Analysis tracking performance are performed using Maximum Tracking Error (MTE) and Root Mean Square Error (RMSE).

CHAPTER 2

LITERATURE REVIEW

2.1 Introduction

For machine tool applications, researchers have been experimenting with different controller architectures since the 1990s with the goal of boosting performance through increased tracking, stability, friction and disturbance mitigation. A common tool in engineering, CNC milling machines are the subject of this paper. The device consists of a table with mechanical and electrical components that enable mobility. The study examines the mechanical drive system and identifies typical disruptions. The performance of the machine is greatly impacted by milling disturbances, especially those involving friction and cutting forces. The research looks at remedial measures, with a special emphasis on decreasing force compensation. PID controllers are widely utilized in both business and research however; to better manage disturbances, researchers frequently merge with adaptive components. Proportional, integral, and derivative gains are all included in the PID controller, which is well-known for being simple to build and use. Potential improvements to the PID controller are suggested by the evaluation, including the addition of a conditional integrator, NPID controllers, or cascade P/PI controllers.

2.2 Mechanical Drive System

Using a CNC milling machine as an example, the mechanical drive system is a critical part of machine tool applications. Based on various investigations, a variety of drive mechanisms are described, including ball screw drives, linear direct drives, rack and pinion drives, and piezoelectric drives. Ball screw drives are recommended since they are less expensive and use a servo motor. To prevent backlash effects, the system has thrust bearings, a nut with flowing balls, and a preloaded nut. Machine tools get direct linear motion from the linear drive, which acts as a linear engine. In contrast to ball screw drives, linear drives do not use a screw or nut, enabling the cutting load to provide direct force to

the electrical motor. Although linear drives perform well in terms of speed and acceleration, they are less able to withstand disturbance forces such as cutting force and friction strength due to their low stiffness. Conversely, ball screw drives are advised for machine tools with significant disturbance forces due to their high rigidity, which guarantees accurate alignment.

2.3 Disturbance in Drive System

Cutting force and friction force have an impact on the disturbance in a machine tool's drive system, as stated by Jamaludin et al. (2006). These disruptive forces, in particular the friction force produced as the ball screw drive moves, might affect the machine tool's tracking performance. Friction force builds up due to rolling behavior's dynamic friction, and axis direction changes have the potential to intensify this force even more. According to Jamaludin et al. (2009), friction force causes quadrant faults in the control system during motion reversal, which lowers machine tool tracking accuracy. Cutting force is another important disruption when it comes to a CNC milling machine, which is used for the cutting process while shaping workpieces. Abdullah (2014) highlights the significance of examining the machine's reaction to cutting force while taking important variables like feeding rate, spindle speed, and cutting depth into ac- count. The formulae (Equations 2.1 and 2.2) relating cutting force, spindle speed, and feed rate are presented by Kalpakjian and Schmid (2001). Equation 2.1 shows that the spindle speed of the cutting tool and the cutting speed are directly correlated, meaning that faster cutting speeds require faster spindles.

$$N = \frac{v}{\pi d} \tag{2.1}$$

Where,

N = Cutting Spindle Speed (revolution per minute, rpm)

v = Cutting speed or feed rate (mm/min)

π = Pi (radian)

d = Diameter of the cutting tool (mm)

According to Equation (2.1), the cutting tool spindle speed is directly related to the cutting speed. As a result, the formula suggests that increasing the cutting speed or feed rate demands increasing the cutting tool spindle speed. When using a cutting tool of the same size, the result would be inverted. Therefore,

$$f = \frac{v}{Nn} \tag{2.2}$$

Where;

f = Feed per tooth (mm/tooth)

n = Number of teeth on the cutting tool

Likewise, Equation (2.2) shows that the feed per tooth is proportional to the cutting speed. An increase in cutting speed corresponds to an increase in feed per tooth, whereas a drop in cutting speed corresponds to a decrease in feed per tooth. The feed per tooth, on the other hand, is inversely related to the cutting tool spindle speed and the number of teeth on the cutting tool. As a result, Denkena and Boujnah and Boujnah (2018) underlined the need of parameter selection to prevent the cutting tool from breaking or deflecting. Furthermore, Equation (2.3) defines cutting force as the ratio of cutting power to cutting speed, a term previously used in works by Kalpakjian, Schmid (2001), Palanivendhan (2014), and CarrLane (2019).

$$F_c = \frac{P_c}{v} \tag{2.3}$$

Where;

F_c= Cutting Force (KN)

P_c = Cutting Power (KW)

v = Cutting Speed (m/Min)

2.4 Cutting Force Analysis Method

The milling machine cutting process is prone to various disturbance forces, with cutting force being a prominent factor. (2018) claims that noise produced during cutting has a negative impact on surface quality and shortens the cutting tool's lifespan. According to Yao et al. (2018), system performance can be improved by evaluating the

behavior of the cutting process using sophisticated cutting techniques. Furthermore, Wanet al. (2016) presented the direct force measurement and indirect force measurement approaches to cutting force model creation. A table dynamometer is used in the direct force measuring technique to measure cutting forces during turning, milling, and grinding operations. Using Dynoware software connected to the machine through a table dynamometer adapter, Halim et al. (2017) recorded cutting force values throughout milling. This technique was made easier by the clamps holding the work piece in place (Matsumura, Tamura, 2017). Cutting force behavior was investigated by researchers such as Huang et al. (2007), Scippa et al. (2015), and Bolar et al. (2018) at different feed rates, spindle speeds, cutting depths, and tool sizes. During the system's controller design phase, these characteristics play a critical role in determining the cutting behavior and in establishing the control scheme. An alternative is provided by indirect techniques of measuring cutting force, which use a few sensors to identify physical events in the system like displacement or current. This approach is favored over direct force measurement for its cost-effectiveness. Wan et al. (2016) pointed out a disadvantage, stating that environmental conditions such as temperature and humidity can impair measurement accuracy. Capacitance dis- placement sensors are often used for indirect force measurement, as demonstrated by Albrecht et al. (2005)'s Kalman filter system. The capacitance displacement sensor, which is often located at the main cutting spindle in machine tools, acts as a spindle speed compensation in this method, therefore increasing the sensor's bandwidth.

2.5 Cutting Force Disturbance Compensation Technique

A controller can be designed to serve as a compensator within the system's control scheme to offset the influence of cutting force in machine tools. When paired with a disturbance observer, this designed controller improves tracking performance robustness. By integrating with the controller, the disturbance observer, a dependable component, aids to obtaining the necessary tracking performance. According to Jamaludin et al. (2016), the disturbance observer is skilled at estimating the movement and behavior of disturbances within a control system. Anang et al. (2017) used an NPID controller to resolve cutting force disturbances in the XYZ ball screw drive table in a prior work. The addition of a nonlinear function to the traditional PID controller improves tracking

performance. Anang et al. (2018) used two kinds of NPID controllers: one based on U_i and k_d and the other on K(e). The study indicated that developing a unique control algorithm may improve machine tool tracking performance, assuring precision and exact placement. To examine the efficacy of the proposed controller, it was compared to existing ones throughout the validation phase. Abdullah introduced and investigated a novel control algorithm known as Nonlinear Cascade Feedforward (NCasFF) in 2014. Following that, the tracking performance of NCasFF was compared to that of the established P/PI cascade controller and NPID controller. The plant in the experiment was an XYZ ball screw drive table with a fixed disturbance force. The Fast Fourier Transform (FFT) method was used for the analysis and comparisons. The results showed that NCasFF's tracking performance outperformed both benchmark controllers. Koren and Lo (1992) investigated various control mechanisms such as the P con- troller, PID controller, Zero Phase Error Tracking Controller (ZPETC), and Cross Coupling Controller (CCC). These controllers were subjected to simulation and experimentation on a CNC milling machine. Using the ZPETC necessitates a thorough under- standing of the system's dynamic behavior, as it employs the concept of cancelling poles or zeros, which makes meeting the desired requirements difficult due to differences between the model and the actual plant. In simulation results with disturbance force, the CCC controller, which included the contour error model and control law, outperformed the P and ZPETC controllers. The researchers came to the conclusion that the CCC technique is the best option for a servo motor algorithm.

Kim and Kim created an adaptive controller for the XYZ ball screw drive table in 1996. The adaptive system, which included a controller adjustment mechanism, robust servo controller, model parameter estimator, and system model, was subjected to x- axis model analysis via simulation and experimentation. The frequency response of the model was examined further. Cutting forces calculated indirectly from current were compared to those measured by the Kistler table dynamometer. The results showed an 8noticed during changes in cutting tool direction a difficulty that was overcome by adjusting the timing for each movement change. The adaptive controller demonstrated improved performance, perhaps improving accuracy and stability.

Choi et al. (1999) developed the Model-Based Disturbance Attenuator (MBDA) as a disturbance reduction technology, which is used in conjunction with a cascade P/PI

controller applied on a CNC machine. The controller's performance was compared to three other methods: (i) cascade P/PI, (ii) Disturbance Observer (DOB), and (iii) Simplified ARC (SARC). The evaluation focused on the sensitivity and complementary sensitivity created during disturbance reduction, as well as how measurement noise was handled. When fitted with an extra Disturbance Observer (DOB), the cascade P/PI controller outperformed both the proposed controller and the Simplified ARC (SARC) in the low-frequency band. As a result, the performance of the cascade P/PI controller suffers in the presence of system disturbances. The superiority of MBDA and SARC in control system performance is obvious in their step responses, which demonstrate improved transient reactions when compared to the other approaches. The Model-Based Disturbance Attenuator (MBDA) has been proven as a viable approach for attenuating system disturbances.

Altintas et al. (2000) developed an adaptive Sliding Mode Controller (SMC) for high-velocity systems, which provides resilience in moderating disturbance forces usually created by equipment, such as friction and cutting forces. The design of the controller included critical processes such as choosing the sliding surface and finding the Lyapunov function, which is critical for stability, especially in nonlinear systems. When compared to a pole placement controller with feedforward friction and servo dynamic compensation, the suggested SMC offers simplicity with a single adaptation and feedback gain.

The pole placement controller, on the other hand, needs greater calculation and exact modelling. Utilizing Quantitative Feedback Theory (QFT), Kim et al. (2003) developed a robust force controller tailored for cutting applications. The new algorithm, crafted through modeling and experimentation, surpassed the performance of the basic robust controller, yielding superior outcomes. Additionally, Landers et al. (2004) assessed a range of machine controllers, including nonlinear, adaptive, linearization, robust, and log transform, employing both simulation and experimental approaches. The effectiveness of these controllers was gauged based on criteria such as stability, robustness, and transient performance. A milling machine with preset settings was used to validate the controllers, with a spindle speed of 1500 rpm and a maximum disturbance force of 0.285 KN for cutting 6061 aluminum material. All nonlinear properties inherent in the machining process are accommodated by the nonlinear controller architecture. Because the adaptive controller is complex, it uses a Recursive Least Squares (RLS) approach to calculate the

necessary parameters. The linearization controller, on the other hand, employs a mechanism to turn nonlinear behavior into an approximated linear system. The robust controller assures performance within specified limitations by utilizing the Quantitative Feedback Theory (QFT) principle. Finally, the log transform controller allows the system to adapt a nonlinear property to an additive disturbance equation. The nonlinear, linearization, and log transform controllers were improved with the addition of an integral term and Model Reference Control (MRC) architecture. The experimental results showed that nonlinear and log transform controllers outperformed linearization and robust controllers over a wide range of parameters.

The nonlinear, linearization, and log transform controllers were improved with the addition of an integral term and Model Reference Control (MRC) architecture. The experimental results showed that nonlinear and log transform controllers outperformed linearization and robust controllers over a wide range of parameters. The whole controller architecture is seen in Figure 2.1. The GMS model parameters were determined using different constant velocities, whereas the position controller parameters were determined using an open-loop test. Unfortunately, the inverse-model-based disturbance observer cannot reduce harmonic cutting forces that exceed the controller's bandwidth. As a result, a second-order repetitive controller was implemented to compensate for the harmonics cutting pressures outside of this frequency.

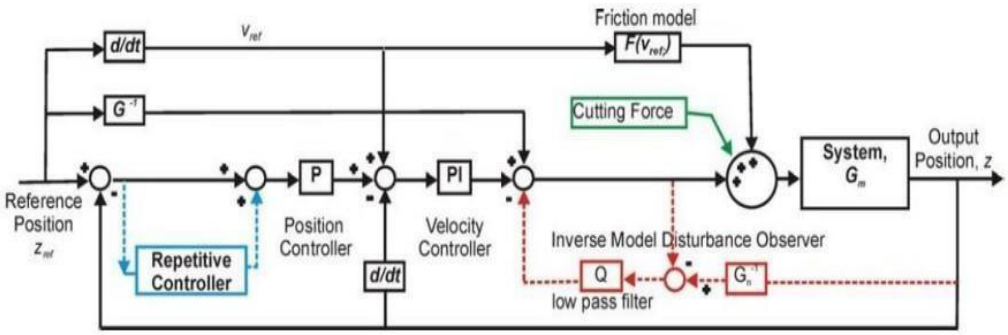

Figure 2.1: The complete control scheme of the position controller (Jamaludin et al., 2008)

A single-axis, high-speed direct-drive mechanism was equipped with a Disturbance Adaptive Discrete-Time Sliding Mode Controller (DADSC), as presented by Altintas and Okwudire (2009). In order to create a stable system that could reduce cutting force

disturbances, the Disturbance Adaptive Discrete-Time Sliding Mode Controller (DADSC) was improved using a disturbance recovery transfer function. Errors between -123 and -133 dB are efficiently reduced by disturbance recovery, resulting in an impressive 350cascade P/PI controller, which includes acceleration and velocity in the feed-forward, were compared. The reference signal's tracking performance is improved by the cascade P/PI controller's feed-forward module. The closed-loop system's motion is not intrinsically reduced by the velocity loop alone, which causes error buildup. As a result, when it came to disturbance rejection, the DADSC performed better than the two controllers. The DADSC's peak error, which was recorded at -140 dB on the measured bode plot, was less than the cascade controller's peak error, which was recorded at -135 dB.

In order to manage the feed rates of cutting tools, Zuperl et al. (2011) created a feed-forward neural adaptive controller and assessed its performance using simulations and tests. This system, in contrast to typical systems that have trouble processing complicated control algorithms smoothly, efficiently accumulates large amounts of data during control planning and execution. Numerous factors were considered in the neural adaptive controller's experimental evaluations, such as the size of the cutting tool, the kind of cutting sample, and the type of cutting surface. The newly constructed controller achieved higher surface quality while maintaining the integrity of the cutting tool, as confirmed by the results, outperforming the conventional one. Kakinuma and Kamigochi (2012) presented a disturbance observer-based automated detection architecture that combines a position controller with a disturbance observer. The linear motor is controlled by the observer, and raising its cut-off frequency reduces disturbance force, but only if it stays within a certain bandwidth to avoid instability. The cutting procedure utilizing a glass workpiece and a micro drill with a 0.1 mm diameter was the main focus of the experimental validation of this control mechanism. The effectiveness of the newly suggested control mechanism was demonstrated by the successful achievement of a smooth surface on the workpiece.

An approach for decreasing disturbance was developed by Hosseinkhani and Ekrorkmaz (2012). It uses a controller architecture that combines a cascade arrangement of a pole-placement controller with Adaptive Feed-forward Cancellation (AFC). This controller was used to reduce interference at three frequencies: 200 Hz for passing frequencies, 50 Hz and 100 Hz for spindle frequencies. To examine the controller's

performance at high-speed frequencies, experiments were carried out. The AFC provided a compelling demonstration of its capacity to lessen cutting force disruptions in the machine tool that was being used. In 2013, Kaan Erkorkmaz and Hosseinkhani created a new disturbance rejection mechanism called Pole Placement Controller and Loop Shaping (PPC+LS). The PD-PID control method was used by the pole placement controller. Using an aluminum 6065 workpiece, the newly developed controller was experimentally tested at various spindle speeds.

A comparative study using cascaded P/PI controllers showed that PPC+LS performs better in terms of disturbance reduction. An active Model Predictive Control (MPC) method was developed by Zhang et al. (2015) with the goal of reducing the effect of noise during the cutting process. This noise shortens the cutting tool's life and increases the likelihood of errors building up throughout manufacturing, which might lower the quality of the finished product. The MPC was evaluated by running many simulations with varying spindle speeds and cutting depths. The obtained findings confirm that noise in the cutting process is successfully reduced by the MPC.

Zhao et al. (2016) addressed the nonlinearity caused by the presence of friction and cutting forces in CNC machines by developing a PI-based controller coupled with Fuzzy Sliding Mode Control (FSMC). Using an IF-THEN format, the fuzzy system was used to calculate the nonlinear system parameters. The purpose of the PI component is to lower input noise and improve steady-state performance. The Lyapunov function was used to evaluate the stability of the controller. Simulation and experimental research were used to validate the new controller's performance, and the outcomes were contrasted with a PI controller combined with simple Sliding Mode Control (SMC). Step responsiveness, noise reduction, and tracking inaccuracy were among the evaluation criteria.

From position error and its rate of change to compensate various system faults. Evaluation included a range of cutting tool spindle frequencies and speeds, including studies using an amplitude of 10 mm. At the 30 second point, cutting forces from various spindle speeds were added. The cascaded fuzzy P/PI controller beat the basic PI controller and the fuzzy PI controller by 70.9 respectively, in benchmarking. An overview of the controllers used by previous researchers to compensate for cutting force disturbances is given in Table 2.1.

Table 2.1: Cutting force disturbance compensation technique summary

Author	Controller	Strength	Weaknesses
Anag et ai.	NPID	• Flexible towards nonlinearity	• More Improvements needed • Complex design
Abdullah	NCasFF	• High flexibility	• User need to master the knowledge of system dynamic behavior
Koren and Lo	CCC	• Good Contouring accuracy • Best selection for servo motor algorithms	• Higher computation load
Kim and Kim	ACC	• Easly embedded into other mechanics	• Long adaptation time
Choi et al.	MBDA	• Simple and intuitive	• Not used widely
Altintas et al., Zaho et al.	SMC	• Adaptive • Widely used in nonlinear application	• Chattering issues • Complex design
Kim et al.	QFT	• Compensates Process effective	• Limited range
Jamaludin et al.	IMBO w repetitive controller	• Compensate harmonics frequency outside bandwidth	• Complex design
Altintas and Okwudire	DADSC	• Good dynamic stiffness	• Error accumulation
Zuperl et al	Feed-forward neural adaptive controller	• Ability to collect large amount of data • Can maintain the quality of cutting tool • Stable	• Complex model
Kakinuma and Kamigoci	Disturbance observer	• Obtained a smooth surface of work-piece	• Involves a lot of parameters and mathematical models
Hosseinkhani and Erkokmaz	AFC	• Produce law tracking error	• Complex design
Hosseinkhani and Erkokmaz	PPC+LS	• Superior in rejecting disturbance	• Robustness not proven • Complex design
Zhang et al.	MPC	• Reduce the noise effect	• Not Proven in Different
Rates et al.	Fuzzy P/PI	• Robust	• Complex way to determine parameters

2.6 Summary

The NPID controller was effectively used in a machine tool application by Abdullah et al. (2015), who also showed that it was more effective than either NCasFF or Cascade P/PI. Using FFT error analysis, the efficacy of these controllers was examined; the NPID controller was effective in correcting mistakes brought on by disturbance force. Kler et al. (2018) demonstrated the superiority of the NPID controller over the PID controller in terms of undershoot and settling time by achieving good results in a photovoltaic system. Rahmat et al. (2012) emphasized that the NPID controller outperforms the PID controller in handling large loads.

Although PID controllers continue to be the standard in machine tool applications due to their simplicity and reliability, their use has grown to include P, PI, PD, and cascade P/PI controllers. PID controller capabilities are further enhanced by the addition of adaptive mechanisms and disturbance compensation strategies, as shown in Figure 2.1.

Applications such as robotics, pneumatic control, and machine tools have all used nonlinear functions and conditional integrators. Based on system requirements and circumstances specified in MATLAB/Simulink software, previous researchers used a variety of conditional integrators. More research is needed in the field of conditional integrator use in PID-based controllers, specifically on an XYZ ball screw drive table. In order to improve machine tool performance in terms of tracking precision and accurate positioning, this thesis proposes using an NPID controller.

CHAPTER 3
METHODOLOGY

3.1 Introduction

This chapter explains the procedural details and methodologies employed in the research. A succinct visualization of the research steps is encapsulated in Figure 3.1. The initial phase of this study involves extracting insights from previous research pertaining to the mechanical aspects of the drive system, the prevalent disturbances in the drive system, and the evolution of controllers. A comprehensive literature review is then conducted to synthesize this information.

Identifying the issues that impede the performance of machine tools in prior studies forms the foundation for crafting problem statements. Subsequently, research objectives are delineated to address these identified problems. The ensuing step involves the validation of a proposed adaptive controller through a simulation process, particularly in the presence of disturbances.

The subsequent phase of the research methodology involves the utilization of the system identification technique to derive the system transfer function, serving as the representation of the plant during the simulation stage. Detailed explanation of the subsequent steps in this methodology is provided in Section 3.3.

All two controllers undergo a consistent approach in terms of simulation with the evaluation based on error analysis metrics, namely Maximum Tracking Error (MTE) and Root Mean Square Error (RMSE). The research workflow is briefly summarized in Figure 3.1.

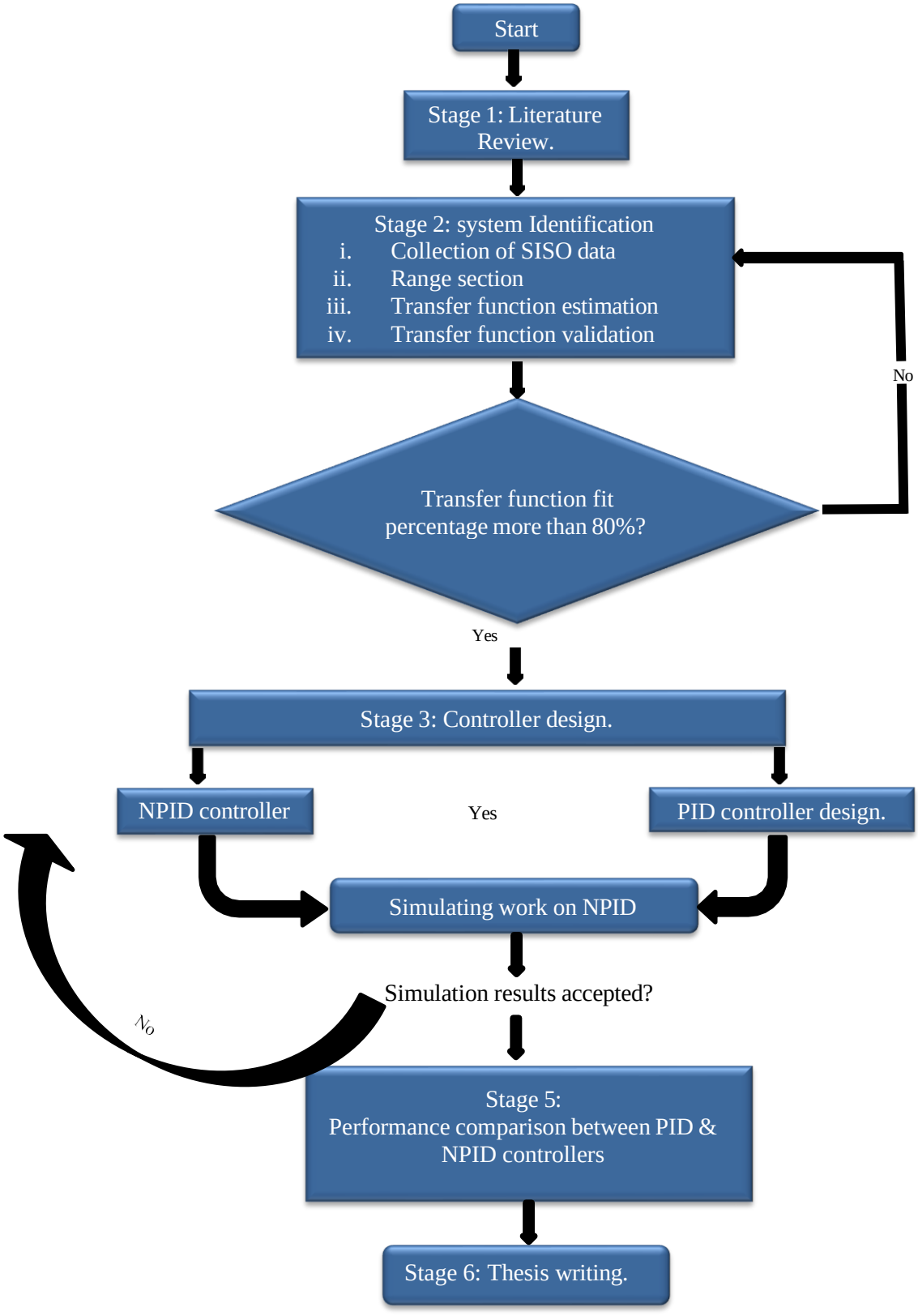

Figure 3.1: Research workflow

3.2 System identification

In the study of Kollár et al. (2006), a technique for obtaining a transfer function that can reproduce a system's dynamic behavior a procedure called system identification was looked at. The primary goal of this study was to create a transfer function that represented the XYZ ball screw drive table machine's plant. Four independent processes comprise the system identification stage:

(i) data collection using single-input single-output (SISO); (ii) data range selection; (iii) transfer function estimation; and (iv) transfer function validation. A thorough explanation of each phase in the system identification process is given in the sections that follow. Notably, Abdullah et al (2012) stressed the importance of the system identification process as the first step in creating a controller for a particular system.

3.2.1 First step: Single-input single-output (SISO) data collection

The first step in system identification, according to Kollár et al. (2006), is gathering (SISO) data. The XYZ ball screw drive table's voltage (V) and output data, measured in millimeters (mm), were the sources of the data. MATLAB, Simulink, and dSPACE were software programs used to gather data. In addition, a control system with an open-loop architecture was created using MATLAB and Simulink software, as shown in Figure 3.2.

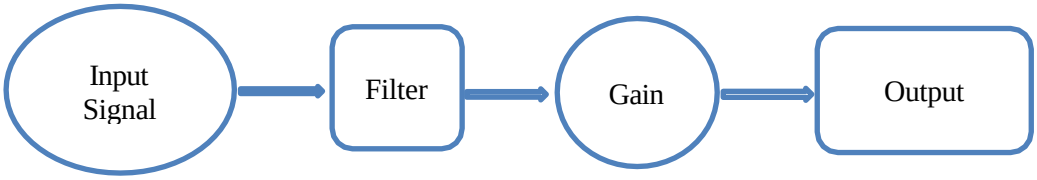

Figure 3.2: System for SISO data collection

The machine limit was exceeded by frequencies, so a low-pass Butterworth filter (20 Hz) was added to the system to filter out frequencies higher than 20 Hz. The gain was used to control the input signal, and it was progressively increased until the signal caused the system to respond. A 300 second SISO data collecting period was used, and the system identification toolbox shown in Figure 3.3 was used to import the data.

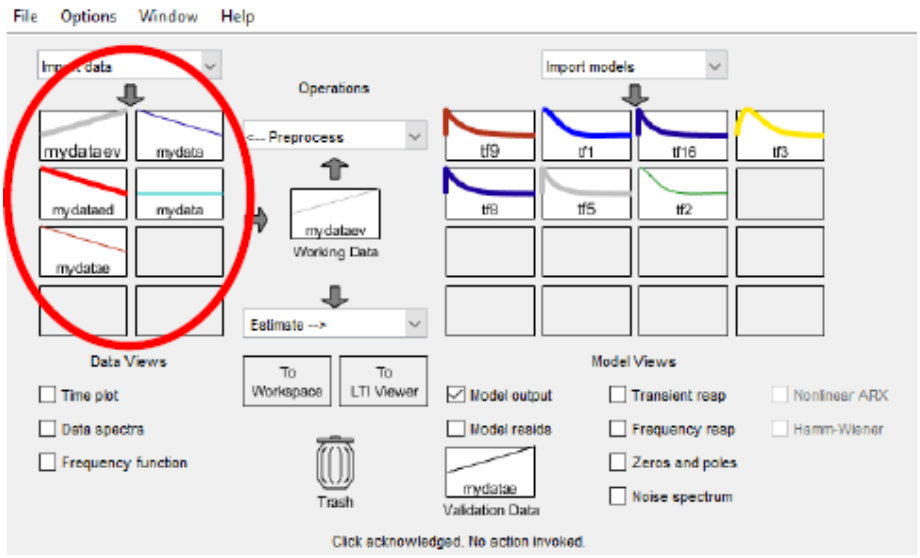

Figure 3.3: Imported SISO data

3.2.2 Second step: Range of data selection

Next, a data range (shown in Figure 3.4) was selected from the SISO data. The preprocess selector made the choosing process easier. To fully capture the overall behavior of the system, the selected signal has to span at least one full cycle. In the next step, the mathematical model is derived using this chosen signal as a foundation.

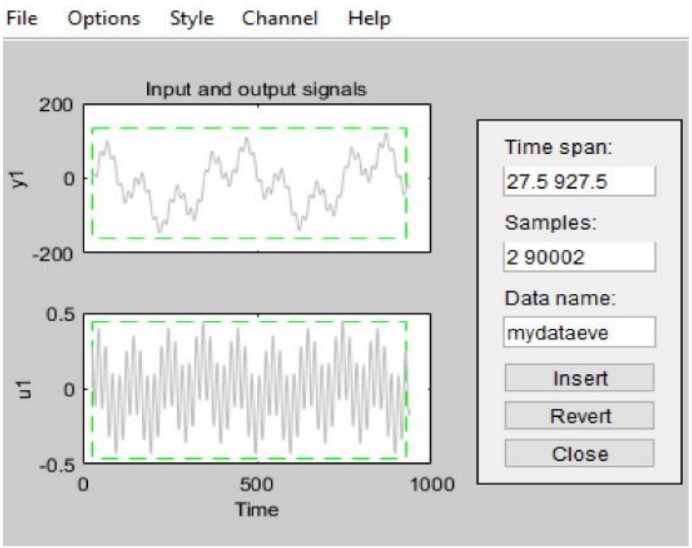

Figure 3.4: Range of data selection

3.2.3 Third step: Transfer function estimation

The rapid start option (shown in Figure 3.5) was selected before the transfer function models were estimated. Because of this property, it is possible to estimate the transfer function using the first half of the signal and then validate it using the second half.

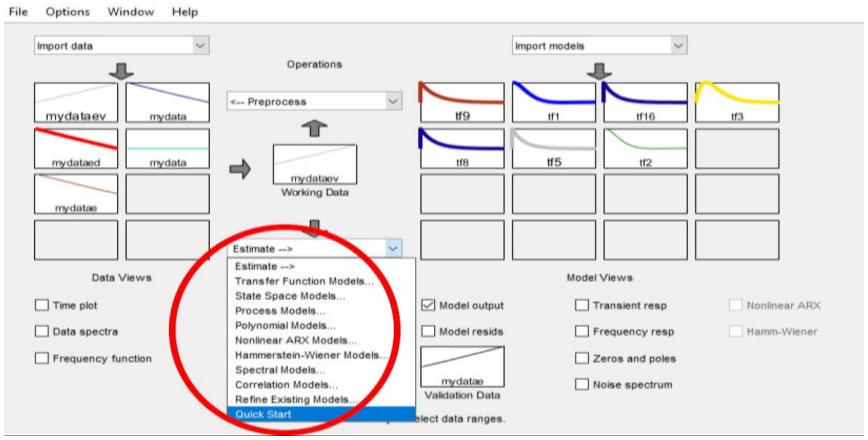

Figure 3.5: Quick start option

The transfer function model was then quickly selected from the estimate menu. The choice of how many poles and zeros to include in the transfer function was made easier by a pop-up window, as shown in Figure 3.6. The identical plant utilized in this study was the subject of earlier research by Junoh et al. (2017) and Maharof et al. (2018), from which a second-order transfer function was derived using two poles and zero zeros. Choosing zeros instead of one or two produced a greater fit %. The transfer function can be expressed in Equation (3.1).

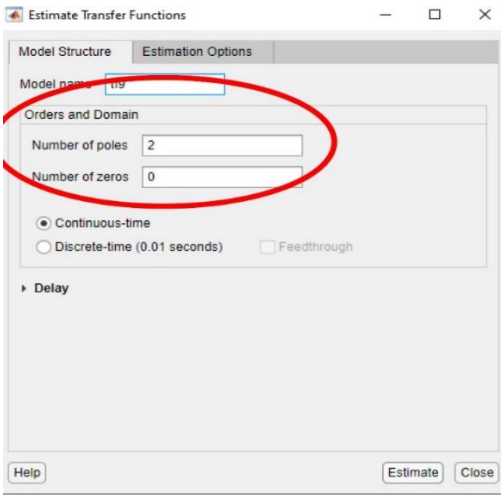

Figure 3.6: The number of poles and zeros selected

$$G_m(S) = \frac{Z(s)}{R(s)} = \frac{A}{S^2+Bs+C} \times e^{-sT_d} \quad (3.1)$$

Where;

$Z_{(s)}$ = Position of the XYZ ball screw drive table

$R_{(S)}$ = Input voltage

A = 225580 mm/V·s^{-2}

B = 125.6s^{-1}

C = 1.414s^{-2}

$e^{-sT}d$ = Transfer function of time delay of 0.0012s

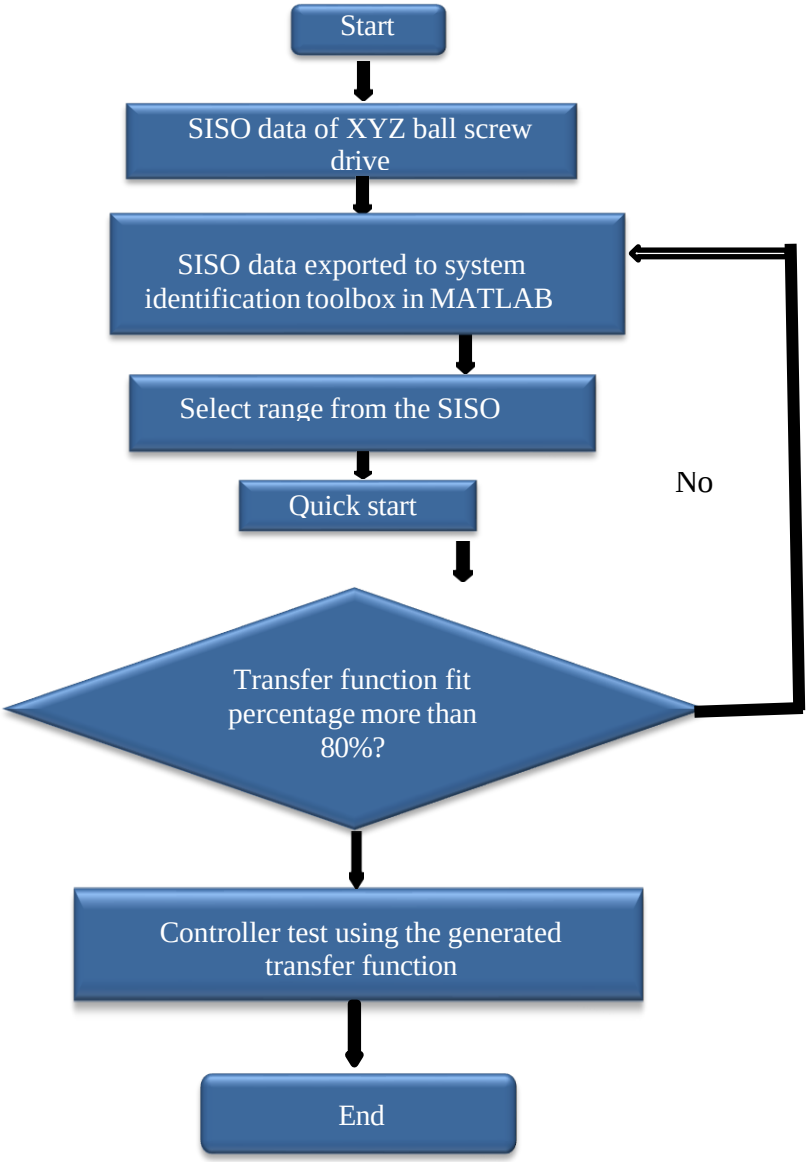

Figure 3.7: The workflow of obtaining the plant transfer function

3.2.4 Fourth step: Transfer function validation

After it was obtained, the transfer function was shown in the model views. A graph of the model output and the fit % was displayed after choosing the transfer function model and ticking the model output box, as shown in Figure 3.10. A fit percentage higher than 80% is considered required for the best similarity to the real plant.

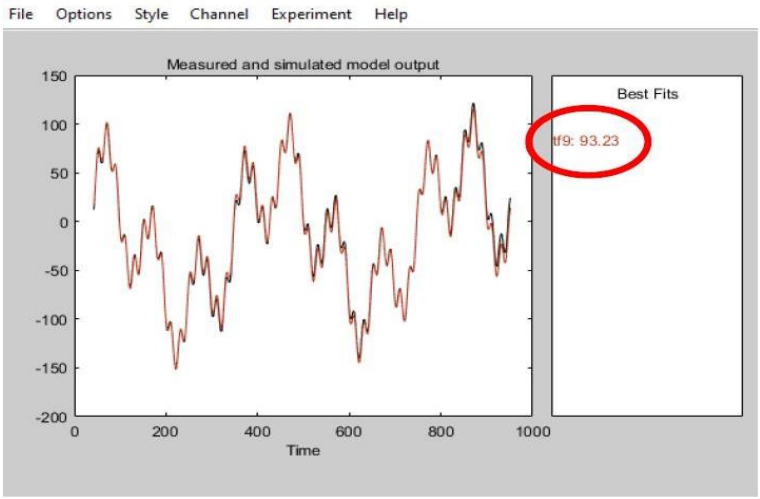

Figure 3.8: Fit percentage obtained

3.3 Cutting Force Disturbance

Cutting force and friction force are two of the many disturbances that can make it difficult to achieve precise positioning in a machine tool. To improve tracking performance accuracy, compensation for disturbances is essential. The tracking performance of the XYZ ball screw drive table system, which is utilized as the machine tool, is greatly influenced by cutting force, which is a noteworthy disturbance factor. Three distinct spindle speeds 1500 rpm and 2500 rpm are used in this study to investigate the effects of cutting force disturbance. Figure 3.9 shows the cutting forces associated with each spindle speed that were obtained from the Kistler dynamometer. The cutting force methodology is consistent with the protocols described by Abdullah et al (2012).

MATLAB/Simulink software is then used to simulate and conduct experiments using the collected cutting force data in order to replicate real cutting force conditions. The cutting force is injected into the system for five seconds during each process.

Figure 3.9 shows that the motor at 1500 rpm produced the maximum disturbance force of 20.28 N, while motors at 2500 rpm produced maximum disturbance forces of 16.77 N. In machine tool applications, cutting force characteristics have a significant influence on Maximum Tracking Error (MTE). As a result, higher cutting force amplitudes are associated with poorer controller tracking performance. Furthermore, an inverse relationship exists between spindle speed and cutting force. Consequently, lower spindle speeds result in higher cutting forces, a hypothesis supported by the formulas derived from Equations (2.2) and (2.3).

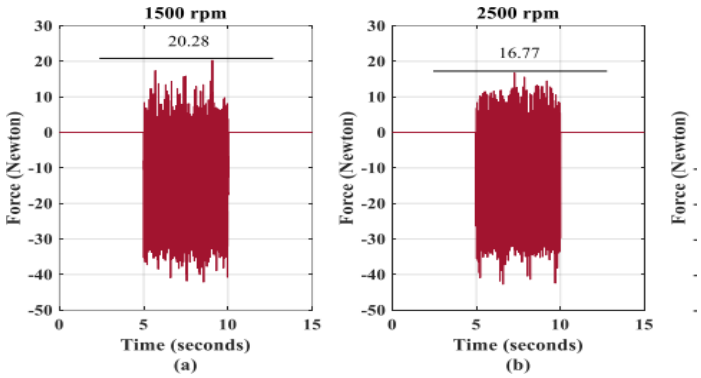

Figure 3.9: Cutting force obtained from Kistler dynamometer for two types of spindles

It is important to note that, as Abdullah (2014) stated, validating the relationship between spindle speed and cutting force is difficult due to the inherent nonlinearity in cutting force behavior, and it cannot be confirmed solely through observation.

Table 3.1: Cutting Force obtained for each spindle speed

Cutting Force	1500 rpm	2500 rpm
Maximum Force (Newton)	20.28	16.77

3.4 Controller Designs

In the following phase, the system's controller is designed with the goal of achieving optimal performance. When integrated into a machine, an ideal controller should have superior tracking capabilities. The PID (Proportional-Integral-Derivative) controller is the industry standard due to its simplicity and applicability. The PID controller, which consists of three essential gains proportional, integral, and derivative, as the name implies is then meticulously tuned into the system.

3.4.1 PID Controller

The PID controller's gains add unique capabilities to system performance. Salim et al. (2013) and Sambariya et al. (2015) found that the proportional gain allows for a commendable rise time, the integral gain reduces steady-state errors, and the derivative gain ensures system stability. Gordon and Erkorkmaz (2013) used gain and phase margin plots to determine PID parameters. In addition, a Nyquist plot was used for parameter identification, taking into account both sensitivity and complementary sensitivity,

ensuring system stability. These analyses were critical in determining the stability of the newly designed controller, and Appendix A contains detailed information on the PID control scheme and control signal.

The frequency domain method was used to determine the optimal parameters for system stability, which included gain margin, phase margin, bandwidth, sensitivity, and complementary sensitivity. Various performance metrics, including Maximum Tracking Error (MTE), number of oscillations, and overshoot, were assessed for various phase margin and gain margin settings. Simulations of the PID controller were performed using MATLAB and Simulink software, with an input signal frequency of 0.2 Hz and a cutting tool spindle speed of 1500 rpm. The MTE was determined as the highest point in the monitoring data, overshoot as the value of the peak in the transient region, and the total amount of oscillations counted prior to reaching the steady-state region.

The optimal PID gains were seamlessly utilized to the NPID controllers, with each controller's specific gains listed in Table 3.2. Equation 3.2 explains how to express the fundamental PID controller as a transfer function. According to Jamaludin et al. (2006), examining an open-loop transfer function yields the gain margin, phase margin, and Nyquist plot. Equation 3.3 depicts this open-loop transfer function, which has been determined as the product of the PID controller function of transfer from Equation 3.2 and the plant transfer function obtained in Equation 3.1 beforehand.

$$G_{PID}(\mathrm{S}) = K_P + \frac{K_I}{S} + K_D \times S \tag{3.2}$$

Where;

K_P=Proportional gain

K_I= Integral gain

K_D= Derivative gain

Open loop transfer function,

$$L = (GPID(s)) \times (Gm(s)) \tag{3.3}$$

$GPID(s)$ = Transfer function of PID controller

$Gm(s)$ = Transfer function of XYZ ball screw drive table

Table 3.2: Proportional gain K_p, Integral gain K_i and Derivative gain K_d

Proportional gain	Integral gain	Derivative gain
1.815	0.002	0.014

The open-loop system model results in an ideal gain margin of 11.9 dB and a phase margin of 62.9º, as shown in Table 3.3 and Figure 3.10. The values follow the rule of thumb of a minimum gain margin of 5 dB and a phase margin of 50º (Abdullah et al., 2013). The gain margin is evaluated at the frequency where the phase variation is 0 dB, whereas the phase margin is determined at 0 dB of the required phase variation, which indicates an impending system instability (Kuo, 1995). The Nyquist plot is an additional tool for evaluating system stability with the specified parameters, and the critical point (-1,0) should not be enclosed (Abdullah et al., 2013). This plot effectively conveys the stability of an open-loop frequency response within the framework of a closed-loop system, emphasizing the relationship between closed-loop system stability and the underlying open-loop system stability. Figure 3.11 depicts the Nyquist diagram generated by the SISO design tool in MATLAB software.

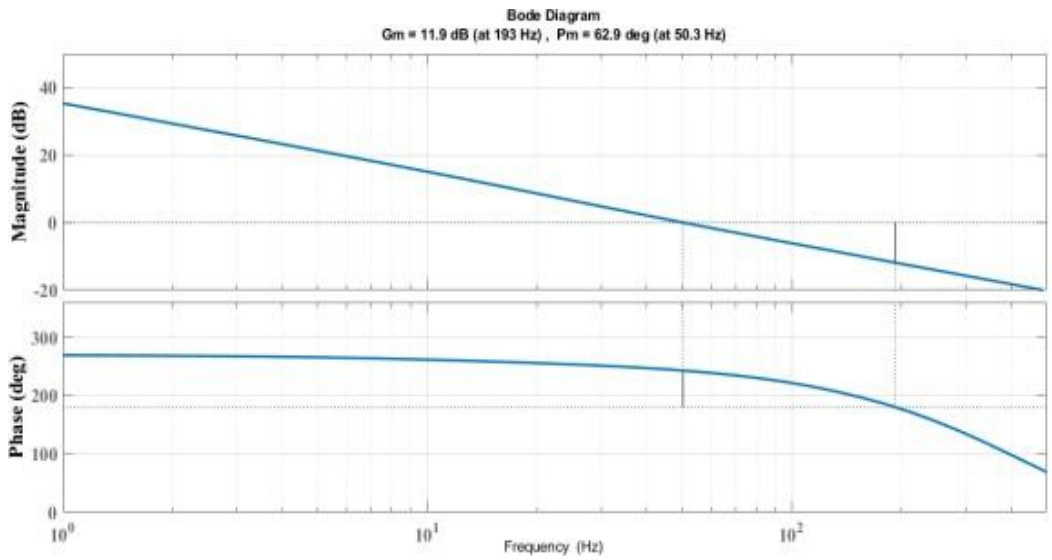

Figure 3.10: Gain maraging and Phase margin bode diagram

Table 3.3: Model of the open-loop system

Model of the open-loop system	
Gain margin	11.9 dB (at 193 Hz)
Phase margin	62.9º (at 50.3 Hz)

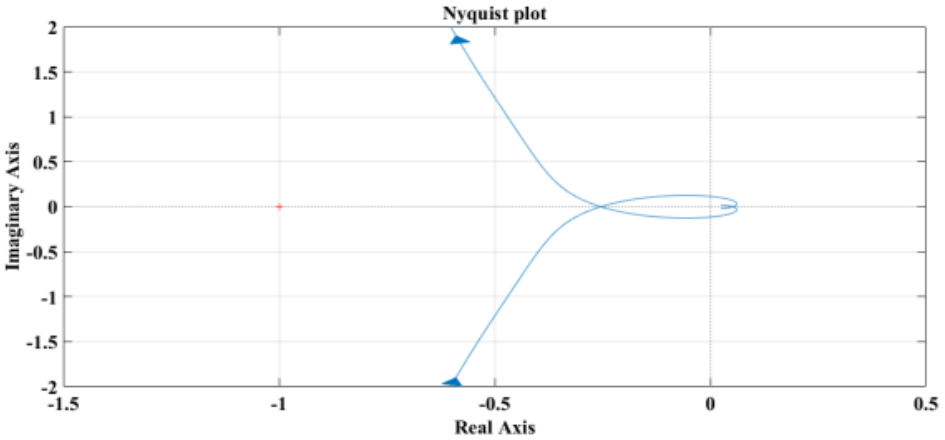

Figure 3.11: Nyquist plot of system

Plotting the sensitivity and complementary sensitivity functions can show the system's stability and resilience (Karer & Škrjanc, 2016). A feedback control system typically acts as a closed-loop system that injects various control signals into the plant based on disturbance errors in order to produce the desired output. Sensitivity and complimentary sensitivity are established as part of the control system feedback operation. Equation (3.4) represents the sensitivity value, while Equation (3.5) represents the complimentary sensitivity. Figures 3.12 and 3.13 show sensitivity and complementary sensitivity plots.

According to Abdullah et al. (2012), peak values for sensitivity and complementary sensitivity must be less than 6 dB and 2 dB, respectively. The analysis of sensitivity and complementary sensitivity are within the specified limits. Exceeding these limits may make the system more vulnerable to noise, disturbances, and errors (Goodwin et al., 2007).

Sensitivity, $$\boldsymbol{S(j\omega)} = \frac{\mathbf{1}}{\mathbf{(1+}\boldsymbol{L}\mathbf{)}} \quad (3.4)$$

Complementary Sensitivity, $$\boldsymbol{T(j\omega)} = \frac{\mathbf{L}}{\mathbf{(1+}\boldsymbol{L}\mathbf{)}} \quad (3.5)$$

Where;

L = open loop of the control system

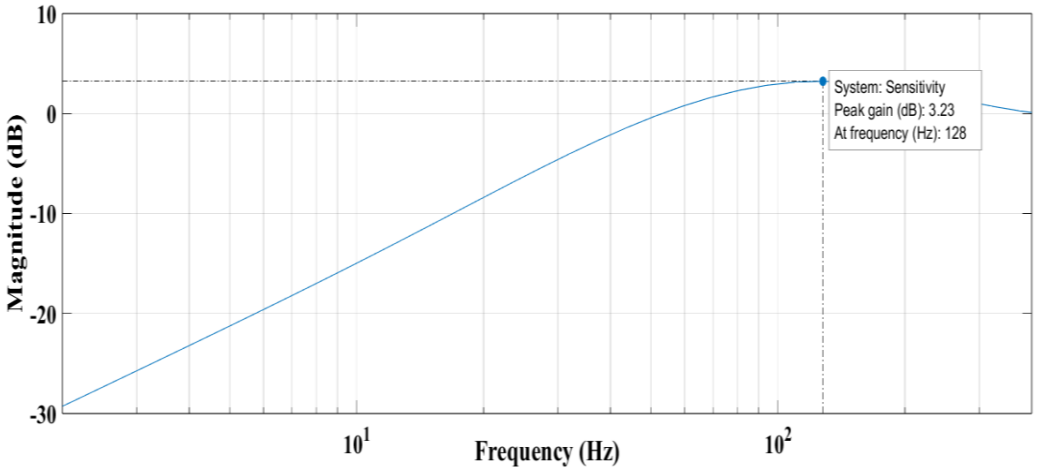

Figure 3.12: Sensitivity plot

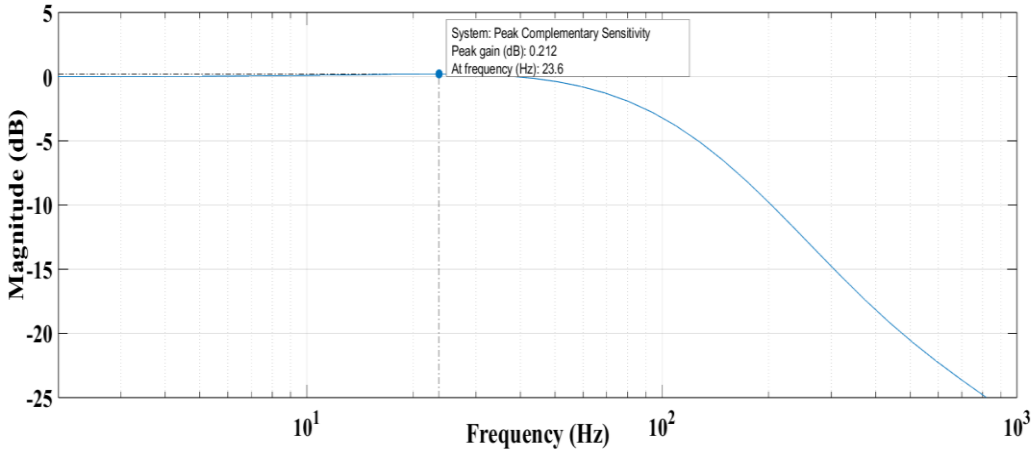

Figure 3.13: Complementary sensitivity plot

Table 3.4: Model of the close-loop system of PID controller

Model of the close-loop system	
Peak value of sensitivity	3.23 dB (at 128 Hz)
Peak value of complementary sensitivity	0.212 dB (at 23.6Hz)

The PID controller's effectiveness on the XYZ ball screw drive table was evaluated based on the parameters specified for each PID gain. Using MATLAB and Simulink software, the PID controller was simulated to see how different PID gains affected its tracking performance. To optimize the performance of the PID controller, each gain was

systematically tuned. In conformity with its nomenclature, the PID controller comprises three gains: P for proportional, I for integral, and D for derivative. The tuning process aims at accomplishing optimal tracking performance while taking into account the individual functions of each gain. Xie et al. (2012) found that a large proportional gain could have a destabilizing effect, which influenced the choice of an appropriate inversely related gain value. In contrast, Sambariya et al. (2015) emphasized the role of the integral gain for minimizing system error, whereas Schellekens et al. (1998) and Salim et al. (2013) noted the derivative gain's stabilizing effect on the system.

3.4.2 NPID Controller Development

The NPID controller introduces several modifications in addition to the PID controller. The NPID controller includes a nonlinear function ahead of the proportional gain (K_p), integral gain (K_i), and derivative gain (K_d). The nonlinear parameter is determined after the PID parameters' values have been set. Drawing on the methodologies used by Salim et al. (2013) and Chiew et al. (2014), a Popov plot is used to determine the maximum permissible range of the nonlinear gain, which is consistent with previous research practices. In this study, the same approach is used. The nonlinear gain adjusts the PID gain based on the magnitude of the tracking error. Figure 3.14 depicts the structural diagram of the NPID controller, and Appendix B describes the Simulink implementation of the NPID component.

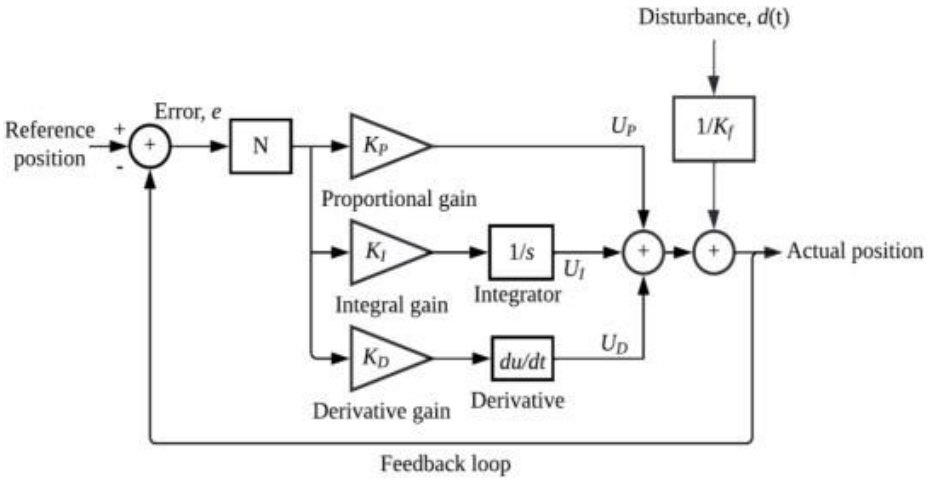

Figure 3.14: Structure of NPID controller

3.5 Research Configurations

This study conducted a comparative analysis of controllers, including the PID controller, and NPID controller. The signal generator produced a sine wave input signal with specific parameters, including an amplitude of 15 mm and frequencies of 0.2 Hz and 0.4 Hz. The sine waveform was used as the input signal for all control schemes to evaluate controller performance and collect tracking error data. In a control system, tracking error is defined as the difference between the input and output signals. Several parameters are critical for determining the input signal. The chosen signal type is a sine waveform with an amplitude of 15 mm, which represents the displacement along the X-axis of the XYZ ball screw drive table. The frequency (0.2 Hz and 0.4 Hz) represents the maximum rotation of the motor in the XYZ ball screw drive table. These specified parameters serve as the input signal for the simulation process, which is injected into the system for 15 seconds. As a result, the simulation only takes into account the first 15 seconds of operation.

3.6 Summary

In summary, this chapter provides a thorough discussion of the methods, procedures, and techniques used throughout the study, presented in a systematic and sequential order. The research is divided into five sections: a literature review of previous studies, the acquisition of the plant's transfer function via system identification, the design and validation of the PID and NPID controllers. The configuration was selected from the previous researcher to obtain the transfer function via system identification and to validate the controller. The system identification process includes data collection for a Single-Input Single-Output (SISO) system, selection of the data range, estimation of the transfer function, and validation of the transfer function. For cutting force experiments, spindle speeds of 1500 rpm and 2500 rpm were used. The collected cutting force data were then injected into the control system scheme during simulation.

CHAPTER 4

RESULT AND DISCUSSION

4.1 Introduction

The results of simulations on a variety of controllers, including the PID controller, and the nonlinear PID (NPID) controller that is used as the standard, are explained in Chapter 4. A sine waveform with an amplitude of 15 mm and frequencies of 0.2 Hz and 0.4 Hz is the signal used for both simulations. This chapter includes a thorough examination of the findings, divided into three sections: Results from the PID controller, the NPID controller, and a comparison of the results for both controllers.

4.2 Maximum Tracking Error

4.2.1 Numerical Validations - PID Controller

The MTE results for each controller are displayed and provides a full description of the PID controller simulation results. MATLAB software was used to carry out the simulation process. After the control framework was built, a sequence of cutting forces with corresponding spindle speeds of 1500 rpm and 2500 rpm were added as disturbance forces to the system. The entire simulation time, which was set at 15 seconds, was spent applying these cutting forces during the time interval of 5 to 10 seconds. The cutting forces were injected into the controller setup before the transfer function.

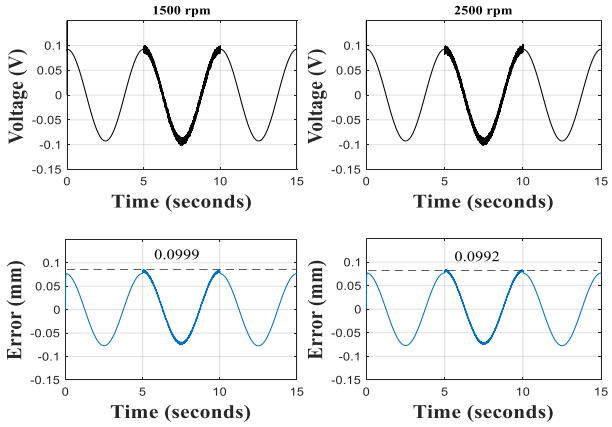

Figure 4.1: Tracking error of PID controller simulated with input signal of frequency 0.2 Hz

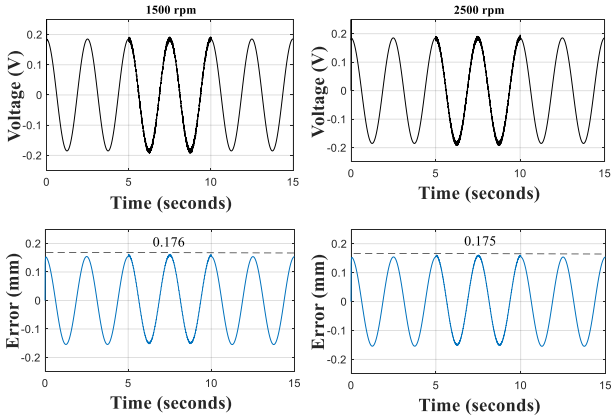

Figure 4.2: Tracking error of PID controller simulated with input signal of frequency 0.4 Hz

Table 4.1: Maximum Tracking Error of PID controller

Spindle Speed (rpm)	Maximum Tracking Error (mm)		Percentage of Error (%)	
	0.2 Hz	0.4 Hz	0.2 Hz	0.4 Hz
1500	0.0999	0.176	0.666	1.173
2500	0.0992	0.175	0.661	1.166

Figure 4.1 shows the simulation results for the MTE of a PID controller at a frequency of 0.2 Hz, and Figure 4.2 shows the results with a frequency of 0.4 Hz. Table 4.1 is a compilation of the MTE values for both frequencies. The difference between the input and output signals is represented by the tracking error, which has a millimeter (mm) measurement.

$$Percentage\ of\ error = \frac{\text{MTE}}{Amplitude} \times 100\% \quad (4.1)$$

PID controller MTE values are 0.0999 mm at 1500 rpm, and 0.0992 mm at 2500 rpm at a frequency of 0.2 Hz. The mean temperature error (MTE) is 0.176 mm at 1500 rpm, and 0.175 mm at 2500 rpm at 0.4 Hz frequency. Equation (4.1) was utilized in the calculation of the error percentages displayed in Table 4.1. Equation (4.1) defines the error percentage as the percentage ratio, given in terms of MTE, between the amplitude of the input signal and the controller. The error percentages for the PID controller at a frequency of 0.2 Hz are 0.666 % at 1500 rpm, and 0.0661 % at 2500 rpm. The error percentages for a frequency of 0.4 Hz are 1.173 % at 1500 rpm, and 1.166 % at 2500 rpm.

4.2.2 Numerical Validations - NPID Controller

Simulink and MATLAB were used in the same way as for the PID controller to simulate the NPID. By applying cutting forces to the system at spindle speeds of 1500 rpm and 2500 rpm, disturbance forces were introduced into the system.

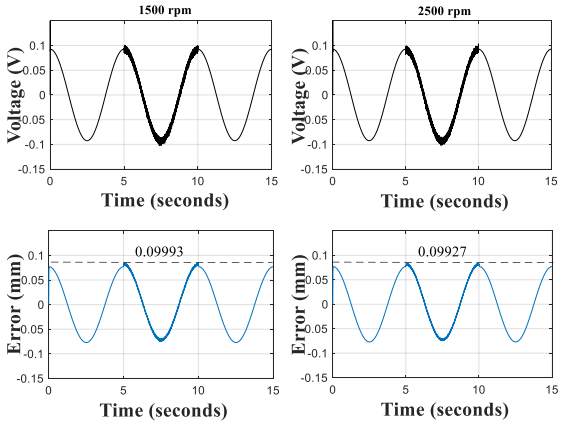

Figure 4.3: Tracking error of NPID controller simulated with input signal of frequency 0.2 Hz

Figure 4.3 displays the MTE results from the simulation of the NPID controller at a frequency of 0.2 Hz. Similarly, Figure 4.4 shows the results of the MTE simulation for the NPID controller at a frequency of 0.4 Hz. Table 4.2 lists the MTE values for each of the two frequencies.

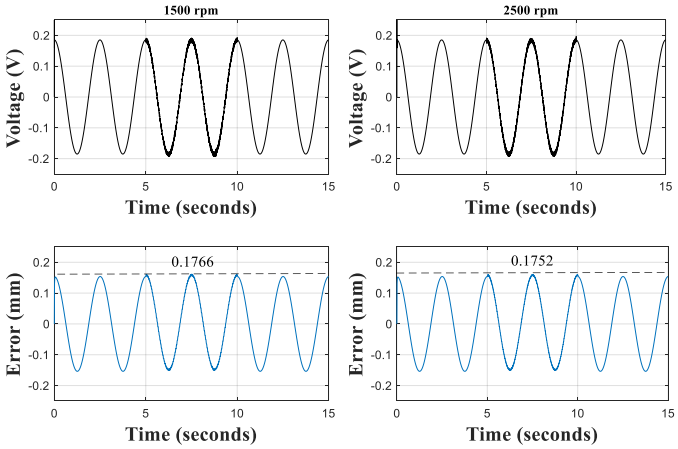

Figure 4.4: Tracking error of NPID controller simulated with input signal of frequency 0.4 Hz

Table 4.2: Maximum Tracking Error of NPID controller for simulation work

Spindle Speed (rpm)	Maximum Tracking Error (mm)		Percentage of Error (%)	
	0.2 Hz	0.4 Hz	0.2 Hz	0.4 Hz
1500	0.09993	0.17660	0.66620	1.17730
2500	0.09927	0.17520	0.66180	1.16800

The MTE for the NPID controller is 0.09993 mm at 1500 rpm, and 0.09927 mm at 2500 rpm at a frequency of 0.2 Hz. The MTE values are 0.1766 mm at 1500 rpm, and 0.1752 mm at 2500 rpm with a frequency of 0.4 Hz. When compared to the PID controller, the NPID controller generates lower MTE values. The percentage of inaccuracy for the NPID controller at 1500 rpm, and 2500 rpm for 0.2 Hz is 0.6662%, and 0.6618%, respectively. The error percentages for 1500 rpm, and 2500 rpm for 0.4 Hz are 1.1773%, and 1.168%, respectively.

4.2.3 Comparison of Maximum Tracking Error

This section compares the simulation results of PID controller and NPID controller based on their MTE outcomes. Figures 4.5 and Figure 4.6 shows the MTE simulation results for the PID and NPID controllers, respectively, while the spindle speed is at 1500 rpm and the frequencies are 0.2 Hz and 0.4 Hz.

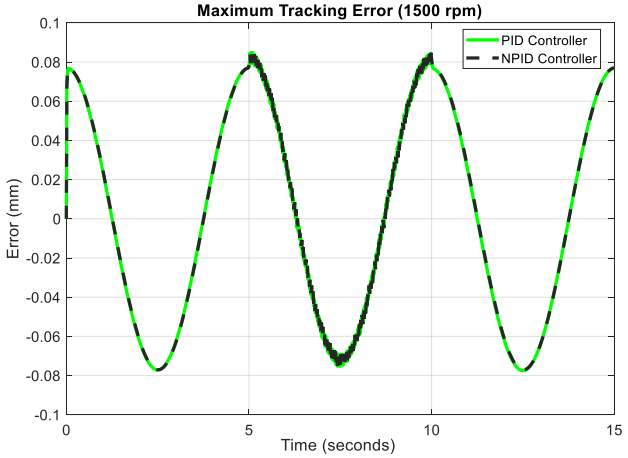

Figure 4.5: Maximum Tracking Error of PID & NPID controllers at 1500 rpm and 0.2 Hz

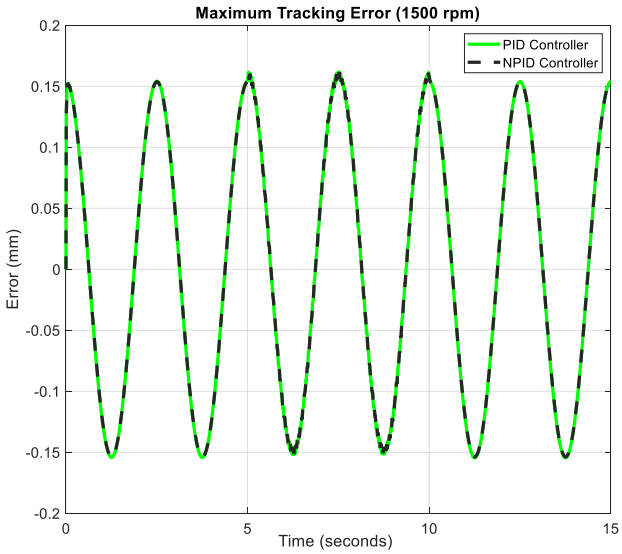

Figure 4.6: Maximum Tracking Error of PID & NPID controllers at 1500 rpm and 0.4 Hz

In comparison to the PID controller's error of 0.09995 mm, the NPID controller obtained a reduced error of 0.09993 mm, according to the MTE data at 1500 rpm and 0.2 Hz frequency. Likewise, at 1500 rpm and 0.4 Hz frequency, the NPID controller demonstrated superior performance, with a reduced error of 0.17660 mm, in contrast to the PID controller's 0.17690 mm error.

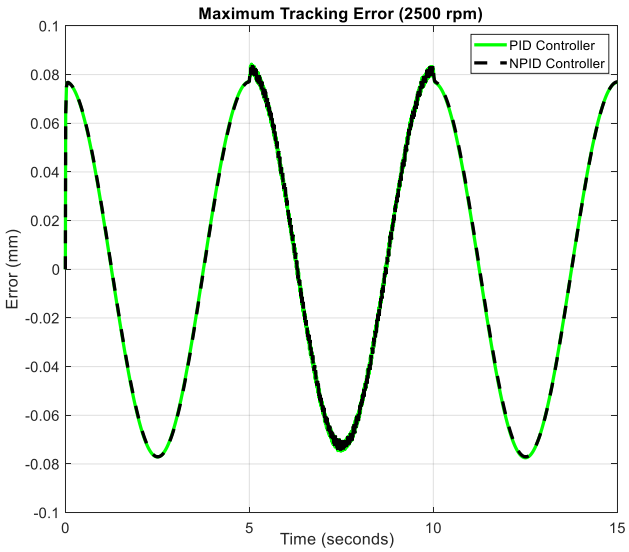

Figure 4.7: Maximum Tracking Error of PID & NPID controllers at 2500 rpm and 0.2 Hz

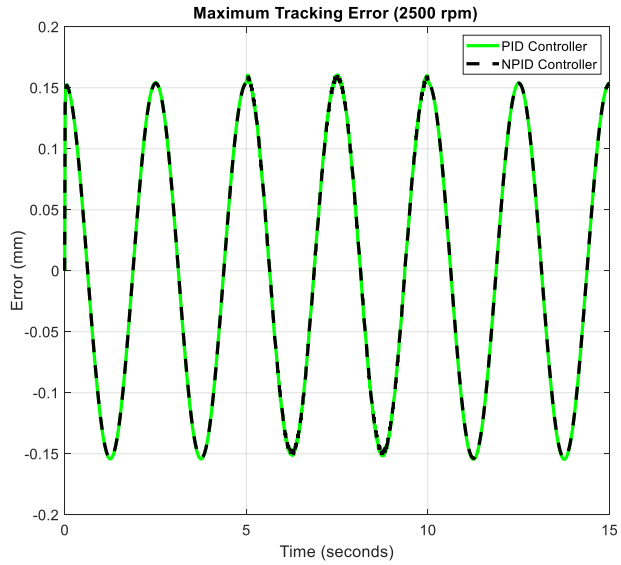

Figure 4.8: Maximum Tracking Error of PID & NPID controllers at 2500 rpm and 0.4 Hz

Figures 4.7 and Figure 4.8, respectively, show the MTE simulation results for the PID and NPID controllers at frequencies of 0.2 Hz and 0.4 Hz in the subsequent scenario, which includes a disturbance from a spindle speed of 2500 rpm. The MTE findings at a frequency of 0.2 Hz and 2500 rpm reveal that the NPID controller had an error of 0.09927 mm, which was less than the PID controller's 0.09920 mm. The PID controller generated an error of 0.17500 mm at 2500 rpm, whereas the NPID controller produced a lesser error of 0.17520 mm at the same frequency of 0.4 Hz. Table 4.3 provides a summary of the simulation's data collection.

Table 4.3: Summary of numerical results

Spindle Speed (rpm)	Input Signal Frequency (Hz)	Maximum Tracking Error (mm)		Percentage of Error (%)	
		PID	NPID	PID	NPID
1500	0.2	0.09990	0.09993	0.66600	0.66620
	0.4	0.17600	0.17660	1.17300	1.17730
2500	0.2	0.09920	0.09927	0.66100	0.66180
	0.4	0.17500	0.17520	1.16600	1.16800

4.3 RMSE Analysis

As the square root of the average of the squared errors in the tracking error data, the Root Mean Square Error (RMSE) is computed. RMSE calculates an average error from each error point in the data, as opposed to MTE, which simply measures the peak error. This section covers the RMSE analysis, expressed in millimeters (mm), at spindle speeds of 1500 rpm and 2500 rpm for both PID and Nonlinear PID (NPID) controllers in addition to the 0.2 Hz and 0.4 Hz input frequencies.

The RMSE, which is given in Equation (4.2), is the square root of the sum of error squares over the total number of errors.

$$RMSE = \sqrt{\frac{\Sigma(e)^2}{n}} \tag{4.2}$$

Where;

e = tracking error data

n = number of tracking error data

Table 4.4 provides the precise RMSE values and the associated error reduction percentages for each controller at various spindle speeds. Figure 4.9 shows the RMSE values for the PID and NPID controllers at a frequency of 0.2 Hz.

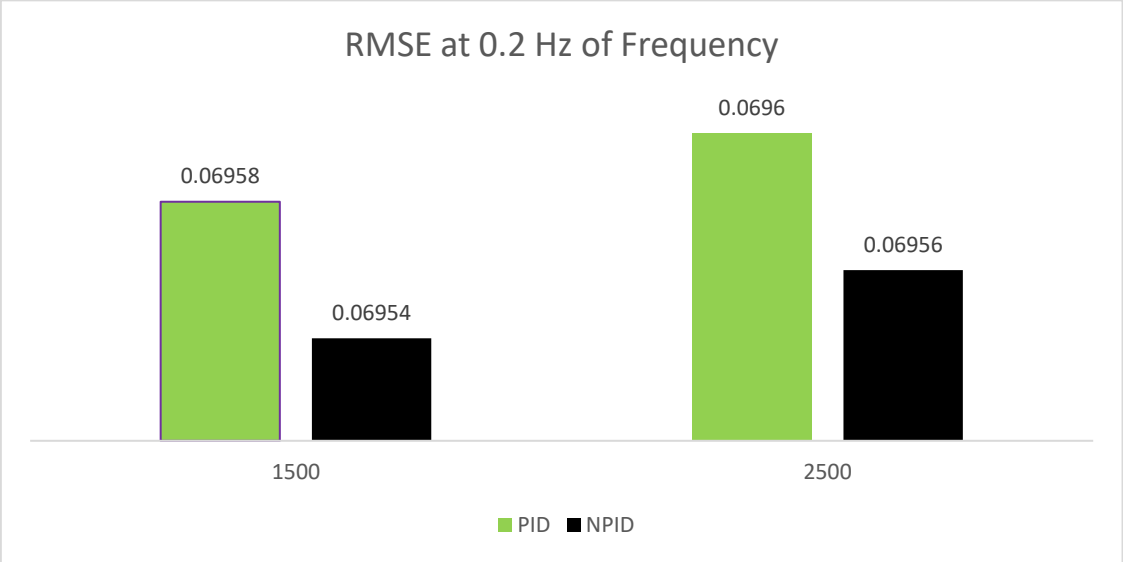

Figure 4.9: RMSE at 0.2 Hz of frequency for PID and NPID controller

The graph presented in Figure 4.9 demonstrates unequivocally how well the NPID controller reduces RMSE. It achieves the lowest RMSE when compared to other spindle speeds, especially at 1500 rpm. Equation (4.2) is used to compute the percentage of error reduction that each controller accomplished, as shown in Table 4.4.

Table 4.4: The value of RMSE and the error reduction percentage for each controller with 0.2 Hz input signal

Spindle Speeds (rpm)	RMSE (mm)		Error Reduction (%)
	PID	NPID	PID vs NPID
1500	0.06958	0.06954	0.05748
2500	0.06960	0.06956	0.05747

Using the values of the two controllers that were to be compared, the percentage of error reduction was computed. When compared to the PID controller, the NPID controller may lower the error by 0.05748% (at 1500 rpm) and 0.05747% (at 2500 rpm). The RMSE

values for the PID and NPID controllers at a frequency of 0.4 Hz are shown in Figure 4.10, and the individual RMSE values and associated error reduction percentages for each controller at various spindle speeds are given in Table 4.5.

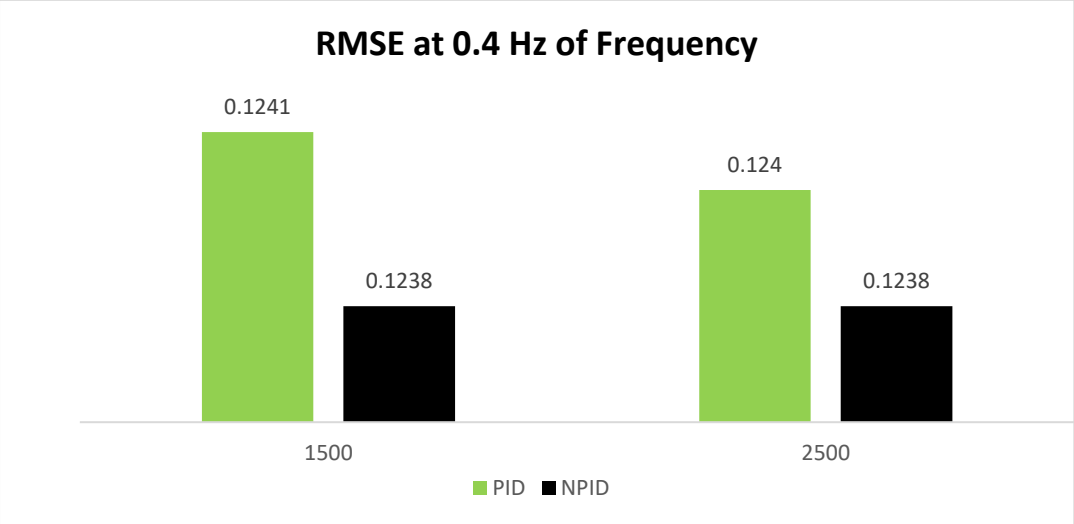

Figure 4.10: RMSE at 0.4 Hz of frequency for PID and NPID

Table 4.5: The value of RMSE and the error reduction percentage for each controller with 0.4 Hz input signal

Spindle Speeds (rpm)	RMSE (mm)		Error Reduction (%)
	PID	NPID	PID vs NPID
1500	0.12410	0.12380	0.24170
2500	0.12400	0.12380	0.16130

The results at a frequency of 0.4 Hz are shown in Figure 4.10. Table 4.5 has more information. The results show that the NPID controller reduces errors by 0.24170% at 1500 rpm and 0.16130% at 2500 rpm when compared to the PID controller.

4.4 Discussion

This section analyzes the results of the PID and NPID controllers with an emphasis on MTE and RMSE. Changes in input frequencies, cutting force spindle speeds, cutting force levels, error kinds and controller types all affect the outcome. There are subsections

specifically for each kind of tracking error, such as Section 4.4.1 for MTE and Section 4.4.2 for RMSE.

4.4.1 Discussions on the MTE Results

The MTE results section is divided into two subsections, Section 4.4.1.1 for the PID controller, Section 4.4.1.2 for the NPID controller, and Section 4.4.1.3 for a comparison of the two controllers, which contain the results for each controller.

4.4.1.1 PID Controller

Based on changes in input frequency and cutting force spindle speed, the PID controller's output is compared. The results of the simulation are shown below:

i. According to the simulation findings, the spindle speed of 1500 rpm produced the maximum MTE.
ii. It was found that an input signal at a higher frequency 0.4 Hz produced a greater MTE than an input signal at a lower frequency 0.2 Hz.

The simulation's MTE at 1500 rpm is the highest, according to Table 4.1. Generally, more interactions between the cutting tool and the workpiece result from a decreased spindle speed, which raises the cutting force disturbances. The data shown in Table 4.1 are consistent with this interpretation. Furthermore, the controller's MTE increased with an increase in the frequency of the input signal. When compared to a 0.2 Hz input signal, a 0.4 Hz input signal produced a higher MTE. Greater tracking errors resulted from the higher frequency signal's longer processing time need because the controller had less time to correct for the higher frequency inaccuracy.

4.4.1.2 NPID Controller

The performance of the NPID controller in terms of MTE is covered in this section. The controller evaluation's results are summed up as follows:

i. greatest MTE value was obtained during simulation at a spindle speed of 1500 rpm.
ii. An input signal of 0.4 Hz produced a greater MTE than an input signal of 0.2 Hz.

Comparing the NPID and PID controllers, similar findings were noted for both. According to Table 4.3, the biggest tracking error happened at 1500 rpm during the experiment. Reduced spindle speeds typically result in more points of contact between the cutting tool and the workpiece, which magnifies the cutting force disturbances. This hypothesis is consistent with the results shown in Table 4.3. In addition, a high MTE was produced by a high frequency input signal, which was also the result of the PID controller. At all spindle speeds, the 0.4 Hz input signal had a greater MTE than the 0.2 Hz input signal. The MTE increases as a result of the controller finding it harder to keep up with the system's speed due to the increased frequency.

4.4.1.3 Comparisons of MTE for PID Controller and NPID Controller

Compared to the PID controller, the NPID controller performed better in compensating for disturbances. Because the PID and NPID controllers had different designs and components, the observations showed that the NPID controller performed better. The NPID controller's N function adjusts the injected gain to the error in the system, improving overall system performance.

4.4.2 Discussions on the RMSE Results

The RMSE findings for the two participating controllers are covered in this section. The results may be summed up as follows:

i. Of all the spindle speeds tested, the cutting force at 2500 rpm yielded the maximum RMSE.

Since both outcomes indicate the same kind of errors, the RMSE and MTE are comparable. But RMSE takes into account every tracking error point, whereas MTE simply takes the tracking error's maximum peak into account. Equation (4.2) was used by the program to produce the RMSE result.

4.5 Summary

In this chapter, the tracking performances of two distinct controllers:

i. The PID controller and NPID controller are shown and discussed.

ii. MATLAB Simulink software was used to simulate and assess the control performances of various controllers.

iii. Maximum Tracking Error (MTE) and Root Mean Square Error (RMSE) were used to compare the two controllers' control performances.

CHAPTER 5
CONCLUSIONS AND RECOMMENDATION

5.1 Conclusion

In order to improve tracking capability in machine tool applications, this research investigates new control formulations. These formulations take cutting forces into account. Its straightforward design and ease of use led to the selection of the PID controller as the main cutting force compensator. But in order to overcome these shortcomings, the PID controller has to be modified and enhanced. The nonlinearity of the system has prompted several researchers to suggest nonlinear PID controllers. Consequently, for the XYZ ball screw drive table, a nonlinear PID controller is suggested and constructed. Simulated testing validates and confirms the controller's capacity to account for the cutting forces within the machine. The design procedure of the suggested controller has three steps. The PID parameters must be determined in the first step. System stability is attained by tuning and analyzing the PID gains using the frequency domain approach.

The results of the two controllers' simulations were covered in the preceding chapter. The plan's transfer function, which came from the system identification method, was used in the simulations. Maximum Tracking Error (MTE) and Root Mean Square Error (RMSE) were the errors computed and examined in this study to assess controller performance. Variations in spindle speed and system frequency can affect these inaccuracies.

The frequency of 0.4 Hz employed in this study produced a bigger inaccuracy than 0.2 Hz. Different spindle speeds also have an impact on tracking error, with greater spindle speeds producing larger inaccuracies. Increased tracking errors are the result of greater cutting forces produced by faster spindle speeds.

REFERENCES

[1] Abdullah, L., 2014. A New Control Strategy for Cutting Force Disturbance Compensation for XY Table Ballscrew Driven System. Ph. D. Dissertation, Universiti Teknikal Malaysia Melaka (UTeM), Malaysia.

[2] Denkena, B., and Boujnah, H., 2018. Feeling machines for online detection and compensation of tool deflection in milling. CIRP Annals, 67(1), 423-426.

[3] Kalpakjian, S., and Schmid, S.R., 2001. Manufacturing Engineering and Technology, 4th ed., New Jersey: Prientice-Hall.

[4] CarrLane., 2019. Machining Operations and Fixture Layout. [online] Available at: https://www.carrlane.com/enus/engineeringresources/technicalinformation/powerworkholding/design-information/machining-operations-fixture-layout.

[5] Jamaludin, Z., van Brussel, H., and Swevers, J., 2006. Tracking performances of cascade and sliding mode controllers with application to a XY milling table. Proceedings of ISMA2006: International Conference on Noise and Vibration Engineering, 1, 81–91.

[6] Jamaludin, Z., Van Brussel, H., and Swevers, J., 2009. Friction Compensation of an XY Feed Table Using Friction-Model-Based Feedforward and an Inverse-Model-Based Disturbance Observer. IEEE Transactions on Industrial Electronics, 56(10), 3848–3853.

[7] Halim, N.F.H.A., Ascroft, H., and Barnes, S., 2017. Analysis of Tool Wear, Cutting Force, Surface Roughness and Machining Temperature during Finishing Operation of Ultrasonic Assisted Milling (UAM) of Carbon Fibre Reinforced Plastic (CFRP). Procedia Engineering, 184, 185–191.

[8] Huang, S., Tan, K.K., Hong, G.S., and Wong, Y.S., 2007. Cutting force control of milling machine. Mechatronics, 17(10), 533-541.

[9] Koren, Y., and Lo, C.C., 1992. Advanced Controllers for Feed Drives. CIRP Annals, 41(2), 689-698.

[10] Kim, T.-Y., and Kim, J., 1996. Adaptive cutting force control for a machining center by using indirect cutting force measurements. International Journal of Machine Tools and Manufacture, 36(8), 925-937.

[11] Kakinuma, Y., and Kamigochi, T., 2012. External sensor-less tool contact detection by cutting force observer. Procedia CIRP, 2(1), 44-48.

[12] Hosseinkhani, Y., and Erkorkmaz, K., 2012. High Frequency Harmonic Cancellation in Ball-screw Drives. Procedia CIRP, 1, 615-620.

[13] Erkorkmaz, K., and Hosseinkhani, Y., 2013. Control of ball screw drives based on disturbance response optimization. CIRP Annals - Manufacturing Technology, 62(1), 387-390.

[14] Kim, S.I., Landers, R.G., and Ulsoy, A.G., 2003. Robust Machining Force Control with Process Compensation. Journal of Manufacturing Science and Engineering, 125(3), 423-430.

[15] Hayashi, K., and Yamamoto, T., 2012. Closed-loop data-oriented design of a PID controller. IFAC Proceedings Volumes (IFAC-Papers Online), Vol. 45, Issue 23, IFAC.

[16] Maslan, M.N., Kokumai, H., and Sato, K., 2017. Development and precise positioning control of a thin and compact linear switched reluctance motor. Precision Engineering, 48, 265-278.

[17] Hama, T., and Sato, K., 2015. High-speed and high-precision tracking control of ultrahigh acceleration moving-permanent-magnet linear synchronous motor. Precision Engineering, 40, 151-159.

[18] Li, R., and Khalil, H.K., 2012. Conditional integrator for non-minimum phase nonlinear systems. 2012 IEEE 51st IEEE Conference on Decision and Control (CDC), 4883-4887.

[19] Liu, Y., Lu, M., Wei, X., Li, H., Wang, J., Che, Y., Deng, B., and Dong, F., 2009. Introducing conditional integrator to sliding mode control of DC/DC buck converter. 2009 IEEE International Conference on Control and Automation, 891-896.

[20] Rahmat, M.F., Salim, S.N.S., Sunar, N.H., Faudzi, A., 'Athif, M., Ismail, Z.H., and Huda, K., 2012. Identification and non-linear control strategy for industrial pneumatic actuator. International Journal of the Physical Sciences, 7(17).

[21] Kollár, I., Pintelon, R., and Schoukens, J., 2006. Frequency Domain System Identification Toolbox for Matlab: Characterizing Nonlinear Errors of Linear Models. IFAC Proceedings Volumes, 39(1), 726-731.

[22] Jamaludin, Z., Jamaludin, J., Chiew, T.H., Abdullah, L., Rafan, N.A., and Maharof, M., 2016. Sustainable Cutting Process for Milling Operation using Disturbance Observer. Procedia CIRP, 40, 486-491.

[23] Junoh, S.C.K., Salim, S.N.S., Abdullah, L., Anang, N.A., Chiew, T.H., and Retas, Z., 2017. Nonlinear PID triple hyperbolic controller design for XY table ball-screw drive system. International Journal of Mechanical and Mechatronics Engineering, 17(3), 1-10.

[24] Gordon, D.J., and Erkorkmaz, K., 2013. Accurate control of ball screw drives using pole-placement vibration damping and a novel trajectory prefilter. Precision Engineering, 37(2), 308-322.

[25] Karer, G., and Škrjanc, I., 2016. Interval-model-based global optimization framework for robust stability and performance of PID controllers. Applied Soft Computing Journal, 40, 526-543.

[26] Goodwin, G.C., Graebe, S.F., and Salgado, M.E., 2007. Control System Design. IEEE Control Systems, 27(1), 77-79.